Low Temperature Physics/Fizika Nizkikh Temperatur, 2017, v. 43, No. 7, pp. 986–990

Examples of superconducting technology application: sensing and interfacing

J. Kunert, R. Ijsselsteijn, E. Il'ichev, O. Brandel, G. Oelsner, S. Anders, V. Schultze, R. Stolz, and H.-G. Meyer

Leibniz Institute of Photonic Technology, IPHT, Jena, Germany
E-mail: ilichev@ipht-jena.de

Received March 6, 2017, published online May 25, 2017

Technological processes for the fabrication of low- and high-T_c Josephson junctions, aimed for certain applications, are described. On the one hand, the integration of low-T_c superconductor digital electronics with superconducting sensor arrays enables input signal processing with quantum limited resolution at millikelvin temperatures. We describe this mixed signal superconductor technology for analogue sensor readout and signal multiplexing for operating temperatures down to 300 mK. On the other hand, by making use of modern high-T_c Josephson junction technology, sensitive magnetometers, which require a modest cooling power, can be developed. Examples of the application of the mentioned processes are shown.

PACS: **85.25.–j** Superconducting devices;
85.25.Am Superconducting device characterization, design, and modeling;
85.25.Cp Josephson devices;
85.25.Oj Superconducting optical, x-ray, and γ-ray detectors (SIS, NIS, transition edge);
74.81.Fa Josephson junction arrays and wire networks.

Keywords: superconducting electronics, Josephson junctions, single flux quantum circuits, superconducting quantum interference filters.

1. Introduction

Superconductor digital electronics was proposed over 30 years ago as a basis for ultrafast devices exploiting subterahertz frequencies. Recently, it becomes clear that superconductor electronics can be potentially used for energy saving implementations related to high-performance computing. Indeed, the energy efficiency of modern computers has become a serious problem due to an extremely fast growth of energy consumption by supercomputers and internet-based systems. The energy dissipation in conventional digital electronics is caused by recharging of the corresponding semiconductor circuits. At the same time the size of transistors continues to decrease, and the number of transistors per chip has enormously grown last decades. The main obstacle to keep progress, for instance by using three-dimensional integration, is energy dissipation.

Here the superconducting electronics, utilizing Josephson junctions as nonlinear elements, has the potential to play an important role in future. Its main advantage is a very small power consumption in combination with a very low noise.

On the other hand, the requirement of low temperatures is a big obstacle to superconducting electronics. The handling of expensive cryogenic liquids as ^{4}He or the need of large refrigerators is unwanted for certain applications. Here, existing technologies of high-temperature superconductors (HTS) can lower the technical demands.

For particular applications existing fabrication technologies can be adjusted to fit specific requirements. Also the intelligent use of well-established technologies can circumvent possible obstacles of the fabrication process. In this paper we present examples for both approaches. The first is the modification of a technological process for low-temperature superconducting (LTS) circuits. The second is devoted to the special design of HTS magnetic sensors, and both fit the need of specific applications.

Low-T_c junctions

Historically two processes for the fabrication of Nb-based superconducting circuits have been developed at the IPHT. The first is motiveted by high-sensitive magnetometry: application of superconducting quantum-interference devices (SQUID) sensors is determined by their relatively low intrinsic noise [1]. Based on those elements we develop complete systems for biomagnetic measurements and geophysical exploration. Additionally we use this technology for testing measurement schemes [2] and mimicking scalable designs for quantum computation [3]. The second is aimed for the application of single flux quantum (SFQ) circuits — digital superconducting electronics [4]. The SFQ technology is provided in frame of the IPHT-based FLUXONICS Foundry [5] — a strategic development based on the European roadmap of superconductive electronics [6]. Parameters of these processes are presented in Table 1.

Table 1. Parameters of existing processes for SQUID, RSFQ and requirements for the new mixed signal process

Parameter	SQUID	RSFQ	Mixed signal
Current density, A/cm^2	70–350	1000	100–200
Resistance, Ω/sq	1	1	4–5
Number of Nb layers	2	3	3
Total layers number	7	10	14
Operating temperature, K	4.2	4.2	0.3–4.2

In this section we present a recently developed technological process [7], which is aimed to analogue sensor readout and signal multiplexing (so-called mixed signal superconductor technology), for operating temperatures down to 300 mK. At the end we will discuss recent results of its first implementation.

Security screening or modern astrophysics methods require a substantial improvement of the detected images. This can be done by increasing the pixel numbers, namely increasing the number of sensors. An integration of superconductor digital electronics together with superconducting sensors enables smart multi-channel sensor arrays. However the engineering effort increases extremely with the number of sensors. Problems are, for example, caused by the thermal load of signal lines, cross talk interferences, and electronics noise contribution.

A solution can be to use frequency division multiplexing [8,9]. For terahertz radiation a particular example is shown in Fig. 1 [10]. The low-temperature platform consists of a sensor array and a multiplexer circuitry. In the best case both parts are on-chip [11]. Digital circuits at room temperature (interface, FPGA, A/D and D/A converters, filters, clock timers) act as interface between the superconducting circuits and a computer, needed for controlling, signal processing, visualization, data storage and human interfacing. In common multiplexing systems, the switches are close to the sensor at a low-temperature level and the controller operates at room temperature. The number of wires from room temperature could be further reduced by placing the controller also at the low-temperature level.

On the base of both the SQUID and the SFQ process a mixed signal superconductor technology has been developed and optimized. Main parameters of these processes are shown in Table 1.

A schematic cross section of the new interface process is shown in Fig. 2, with Josephson tunnel junction, shunt

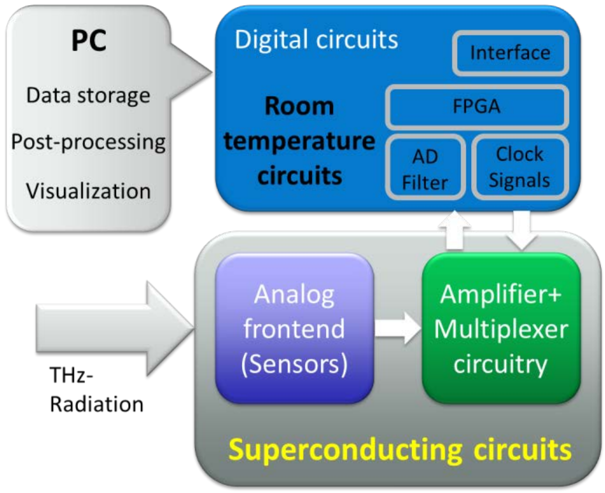

Fig. 1. System scheme multiplexing readout of superconducting sensors.

resistor and bond pad structure. There also the materials and thicknesses of the layers are given.

The layer package consists of three superconductor layers (M0, M1, M2), a resistor layer (R1), a bond pad layer (R2), a layer stack of Nb, Al, Al_2O_3, Nb for the Josephson tunnel junctions (T1), and insulation layers as combinations of Nb_2O_5 and SiO_2 (I0A, I0B, I1A, I1B, I2). A cutting process removes auxiliary electrical connections (CUT) for the anodization step.

The dc-magnetron sputtering is used for deposition of Nb and Al, and reactive ion-etching (RIE) in CF_4 plasma for patterning of Nb. The isolation between Nb layers is realized by anodization for Nb_2O_5 and a SiH_4-based plasma enhanced chemical vapor deposited (PECVD) process

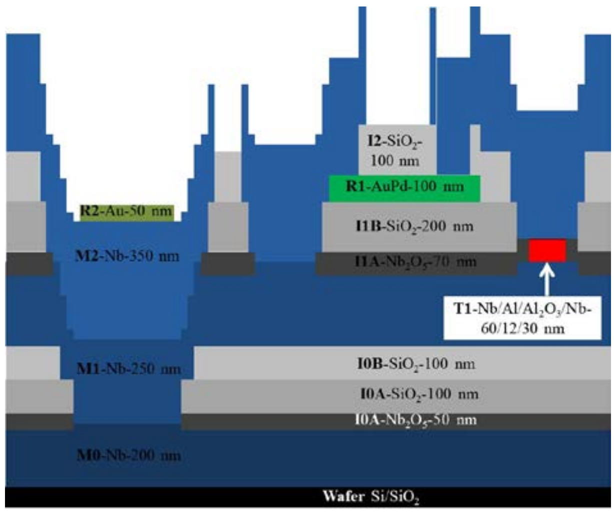

Fig. 2. (Color online) Schematic cross section of the new mixed signal process. The layers materials and thicknesses are given. The superconducting Nb layers are colored in blue, the trilayer forming the junctions in red, the isolation layers in dark and light grey and the normal resistant layers in green.

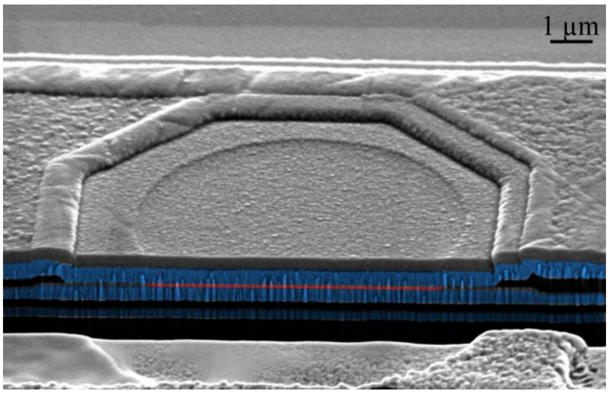

Fig. 3. (Color online) Josephson junction cross section. For better visibility, the thin isolating barrier of Al–Al_2O_3 is highlighted in red, while the Nb layers are colored blue. The black areas correspond to isolation layers. For the SEM picture the chip was prepared by focused ion-beam (FIB). Therefore, an additionally layer (grey on top of Nb) is deposited to protect the structures during FIB milling.

for SiO_2. The SiO_2 is reactive ion-etched with CF_4 and O_2. Laser-based end-point detection controls all RIE processes. Al is patterned by sputter etching with Ar.

Figure 3 shows a Josephson tunnel junction that is formed by a barrier of Al_2O_3 between Nb layers. Nb and Al are in-situ deposited and the surface of Al is oxidized with a thickness of about one nanometer which defines the critical current density J_c. The value of J_c for the mixed signal process is 100–200 A/cm^2. Subsequently Nb is deposited in-situ. The complete stack consists of Nb, Al, Al_2O_3, and Nb. Galvanic anodization of T1 defines the size of the Josephson junctions. The temporary connections for anodization are removed by a subsequent RIE in CF_4 plasma.

To control their damping and suppresses the hysteresis of the tunnel junctions, a shunt resistor layer of AuPd is deposited by sputtering and patterned by lift-off. Because

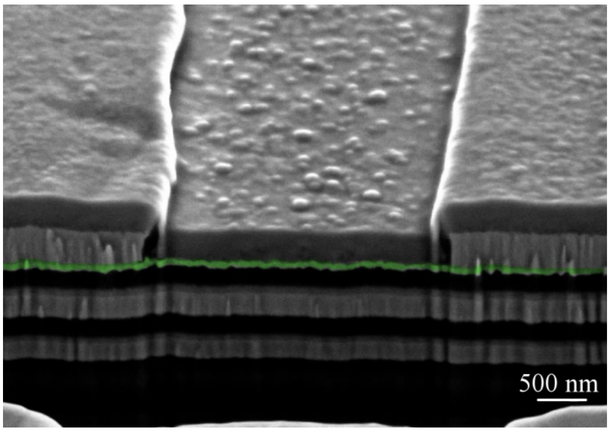

Fig. 4. (Color online) SEM picture of a resistor structure cross section. The FIB milling was similar to Fig. 3. The thin resistor layer is highlighted in green.

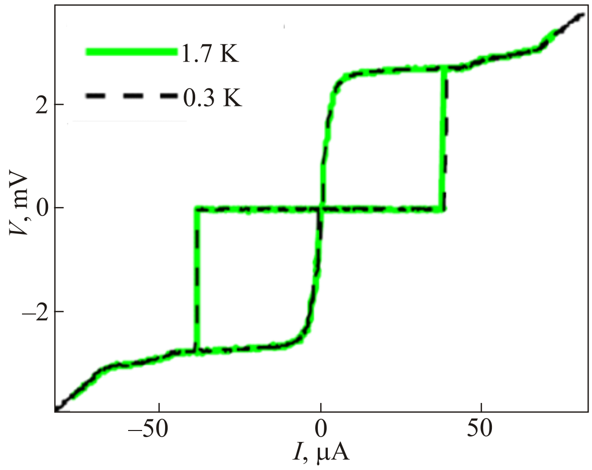

Fig. 5. (Color online) *I–V* plot of a Josephson junction with an area of 20 μm^2 at 1.7 and 0.3 K.

of its temperature independent resistance in the temperature range of interest, this material is chosen. A cross section of a resistor structure is shown in Fig. 4. Finally, the bonding pads are covered by evaporated gold (R2).

To qualify the mixed signal superconductor technology parameters, measurements of the fabricated Josephson junctions at a temperature range down to 0.3 K are necessary. For this measurement a single shot ^{3}He refrigerator with sorption pump technology is used. The samples containing unshunted Josephson junctions are mounted at the 300 mK stage. A superconducting shield suppresses external noise sources. Additionally the control dc lines are filtered by RC-filters at about 1.7 K and at room temperature accompanied by feedthrough filters at room temperature. In a four point setup the current at the junction is ramped and the corresponding voltage recorded.

The results of these measurements at 1.7 and 0.3 K are shown in Fig. 5. The *I–V*-measurements at the two temperatures show the same characteristic. Switching current histograms can, if necessary, reveal the slight temperature dependency of the switching current [12]. From these measurements we also determine the critical current density — for a Josephson junction with a size of 20 μm^2 we find a J_c of 190 A/cm^2. Note, at both measured temperatures the AuPd resistors have the same values, resulting by temperature independence at this temperature range.

Recently we began experiments with a higher integration level of junctions on chip — the measurements are in progress.

3. High-T_c junctions

Potential applications of high-T_c superconductors, motivated mostly by modest cooling power required for keeping the superconducting state, are still restricted by the relatively poor technological abilities. The demonstrated progress for implementation of multilayer processes for

Josephson junction fabrication [13,14] is not enough for the fabrication of scalable superconducting electronic circuits. Nevertheless single-layer structures exploiting so-called grain-boundary junctions can be used for sensitive low-frequency magnetometry [15,16]. Here we present results of fabrication and testing multijunction magnetic field sensors. These sensors are known as superconducting quantum interference filters (SQIFs) [17].

SQIFs are arrays of superconducting loops, with Josephson junctions in each loop and with different sizes of the loops. They can be used for magnetic field measurements in the following way. The superposition of the signals of all these loops results in a large unique delta-like peak at a zero applied magnetic field and almost no modulation at other magnetic fields (see Fig. 6). We have prepared SQIFs by making use of our standard high-T_c technology that is based on $YBa_2Cu_3O_{7-x}$ grain boundary junctions formed on MgO bicrystal substrates. These structures are operated at 77 K. For the arrays 30 to 200 loops are used in serial or parallel configuration or in a combination of both.

First experiments using a standard array of SQUID loops are performed without any pickup loop coupled to the bare SQIF [18,19]. In general, the serial SQIFs work properly and show the expected increase in peak height and a reduction of the magnetic field noise with an increase in the number N of SQUID loops. The parallel SQIFs, however, do not show the expected reduction of the peak width with increasing N and therefore have worse magnetic field noise as expected. This weaker performance is caused by the technologically given spread in the critical currents of the single SQUIDs. This spread causes a redistribution of the currents through the parallel SQUIDs and thereby parasitic flux in the loops. For better field sensitivity, pickup coils are directly or inductively coupled to serial arrays, either on the same substrate or on a separate

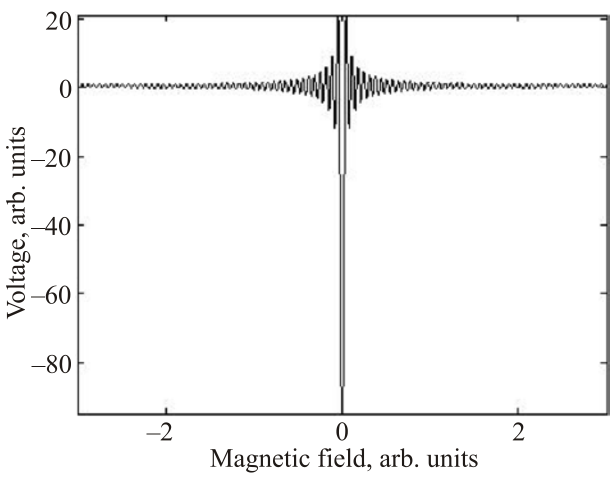

Fig. 6. Theoretical estimate of the voltage-field characteristic of a SQIF formed by 95 SQUIDs. The voltage axis is normalized to the output of a single SQUID.

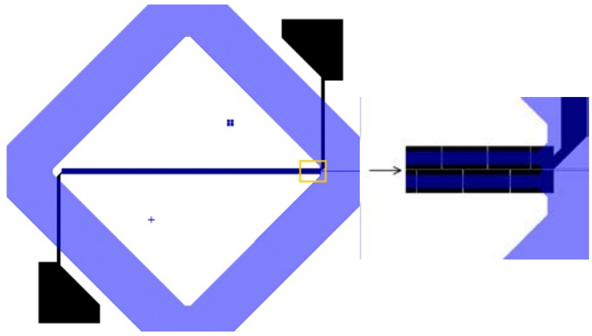

Fig. 7. (Color online) Left: SQIF magnetometer in flip-chip configuration, consisting of a single-layer flux transformer (blue) and a serial SQIF (black). On the right a detail of the SQIF, marked by the yellow rectangle, with 5 out of 95 loops, is shown. The grain boundary is marked by the arrow.

chip flipped to the SQIF. Best results are obtained for flux transformers flipped to a series array of 95 SQUID loops [20], see Fig. 7. We obtain a voltage swing (peak height) of 720 μV, a voltage field transfer factor of 84 μV/nT and a white noise B_n = 65 fT/Hz$^{1/2}$ (107 fT/Hz$^{1/2}$ at 1 Hz). Although B_n is not as low as for modern high-T_c dc SQUIDs [16], SQIFs are still very interesting as magnetic field sensors because they feature (i) relatively high voltage-field transfer function and (ii) a unique voltage peak at zero magnetic fields. A further noise reduction might be obtained by minimizing the inhomogeneity of the Josephson junctions (for instance so-called faceting [21]), namely by using submicron junctions.

4. Conclusion

In conclusion, existing fabrication technologies for superconducting electronics still gives great potential for possible applications. We showed an example for the adjustment of the well-established fabrication process for LTS circuits to fit the specific need of a particular application. Namely the interface of a detector readout to room temperature electronics that is capable of multiplexing. There, adjustments of the working temperature and critical current densities have been experimentally verified. On the other hand, we demonstrated the clever use of well-established HTS technology for the fabrication of sensitive magnetometers. By the use of a serial configuration in the SQIF architecture the influence of the unavoidable spread in the critical current can be reduced.

1. R. Stolz, L. Fritzsch, and H.-G. Meyer, *Supercond. Sci. Technol.* **12**, 806 (1999).
2. E. Il'ichev, Th. Wagner, L. Fritzsch, J. Kunert, V. Schultze, T. May, H.E. Hoenig, H.-G. Meyer, M. Grajcar, D. Born, W. Krech, M. Fistul, and A. Zagoskin, *Appl. Phys. Lett.* **80**, 4184 (2002).

3. V. Zakosarenko, N. Bondarenko, S.H.W. van der Ploeg, A. Izmalkov, S. Linzen, J. Kunert, M. Grajcar, E. Il'ichev, and H.-G. Meyer, *Appl. Phys. Lett*. **90**, 022501 (2007).
4. J. Kunert, O. Brandel, S. Linzen, O. Wetzstein, H. Toepfer, T. Ortlepp, and H.-G. Meyer, *IEEE Trans. Appl. Supercond*. **23**, 1101707 (2013).
5. http://www.fluxonics-foundry.de
6. S. Anders, M.G. Blamire, F.-Im. Buchholz, D.-G. Crété, R. Cristiano, P. Febvre, L. Fritzsch, A. Herr, E. Il'ichev, J. Kohlmann, J. Kunert, H.-G. Meyer, J. Niemeyer, T. Ortlepp, H. Rogalla, T. Schurig, M. Siegel, R. Stolz, E. Tarte, H.J.M. ter Brake, H. Toepfer, J.-C. Villegier, A.M. Zagoskin, and A.B. Zorin, *Physica C* **470**, 2079 (2010).'
7. M. Kiviranta, O. Brandel, L. Grönberg, J. Kunert, S. Linzen, N. Beev, T. May, and M. Prunnila, *IEEE Trans. Appl. Supercond*. **26**, 1100905 (2016).
8. M. Jerger, S. Poletto, P. Macha, U. Hübner, A. Lukashenko, E. Il'ichev, and A.V. Ustinov, *Europhys. Lett.* **96**, 40012 (2011).
9. M. Jerger, S. Poletto, P. Macha, U. Hübner, E. Il'ichev, and A.V. Ustinov, *Appl. Phys. Lett*. **101**, 042604 (2012).
10. V. Zakosarenko, M. Schulz, A. Krueger, E. Heinz, S. Anders, K. Peiselt, T. May, E. Kreysa, G. Siringo, W. Esch, M. Starkloff, and H.-G. Meyer, *Supercond. Sci. Technol.* **24**, 015011 (2011).
11. T. May, V. Zakosarenko, E. Kreysa, W. Esch, S. Anders, L. Fritzsch, R. Boucher, R. Stolz, J. Kunert, and H.-G. Meyer, *IEEE Trans. Appl. Supercond.* **15**, 537 (2005).
12. G. Oelsner, L.S. Revin, E. Il'ichev, A.L. Pankratov, H.-G. Meyer, L. Grönberg, J. Hassel, and L.S. Kuzmin, *Appl. Phys. Lett*. **103**, 142605 (2013).
13. P.V. Komissinski, E. Il'ichev, G.A. Ovsyannikov, S.A. Kovtonyuk, M. Grajcar, R. Hlubina, Z. Ivanov, Y. Tanaka, N. Yoshida, and S. Kashiwaya, *Europhys. Lett.* **57,** 585 (2002).
14. I. Bozovic, G. Logvenov, M.A.J. Verhoeven, P. Caputo, E. Goldobin, and T.H. Geballe, *Nature* **422,** 873 (2003).
15. E. Il'ichev, L. Dorrer, F. Schmidl, V. Zakosarenko, P. Seidel, and G. Hildebrandt, *Appl. Phys. Lett*. **68,** 708 (1996).
16. M.I. Faley, U. Poppe, K. Urban, Yu.V. Maslennikov, A. Gapelyuk, B. Sawitzki, and A. Schirdewan, *Appl. Phys. Lett.* **81**, 2406 (2002).
17. J. Oppenländer, T. Träuble, Ch. Häussler, and N. Schopohl, *IEEE Trans. Appl. Supercond*. **11**, 1271 (2001).
18. V. Schultze, R. IJsselsteijn, H.-G. Meyer, J. Oppenländer, Ch. Häussler, and N. Schopohl, *IEEE Trans. Appl. Supercond.* **13**, 775 (2003).
19. V Schultze, R IJsselsteijn, R Boucher, H.-G. Meyer, J. Oppenländer, Ch. Häussler, and N. Schopohl, *Supercond. Sci. Techn*. **16**, 1356 (2003).
20. V. Schultze, R. IJsselsteijn and H-G. Meyer, *Supercond. Sci. Techn.* **19**, S411 (2006).
21. E. Il'ichev, V. Zakosarenko, R.P.J. IJsselsteijn, H.E. Hoenig, H.-G. Meyer, M.V. Fistul, and P. Müller, *Phys. Rev. B* **59**, 11502 (1999).